

A Thesis
on
OPTICAL AND STRUCTURAL PROPERTIES OF Tb DOPED CdS
NANOPARTICLES

(Submitted in partial fulfillment of requirement for the award of the)

Degree of
Master of Science (M.Sc.) in Physics

Submitted by
Shivani Jindal
Regn. No: 301304009

Supervisor
Dr. N. K. Verma
Senior Professor



School of Physics and Materials Science

Thapar University, Patiala 147 004

July 2015

CERTIFICATE

This is to certify that the report entitled “**Optical and structural properties of Tb-doped CdS nanoparticles**” submitted by **Shivani Jindal, Roll No. 301304009**, student of (M.Sc.) in Physics, School of Physics & Materials Science, Thapar University, Patiala, was carried out by her under my supervision. She has not submitted this material towards any degree at Thapar University, Patiala or any other university.



(Dr. N. K. Verma)

Supervisor

Senior Professor

School of Physics & Material Science

Thapar University, Patiala - 147 004

Countersigned by:



(Dr. Manoj K. Sharma)

Head & Associate Professor

School of Physics & Material Science

Thapar University, Patiala - 147 004



(Dr. S.S Bhatia)

Dean, Academic Affairs,

Thapar University,

Patiala - 147 004

Acknowledgement

This project report is done as a part of course curriculum. I am really thankful to my erudite and revered guide Dr. N. K. Verma, Senior Professor, School of Physics and Materials Science, Thapar University, Patiala, for his invaluable guidance and meticulous efforts, without which the accomplishment of the task would have never been possible. I am much indebted for his benevolent help, appreciation and co-operation.

I express my cordial thank specially to Miss Kamaldeep Kaur for their ever available guidance and indispensable comments, which helped me to develop and shape this study in the present form. I am also thankful to Miss Imanpreet Kaur and Miss GitanjaliDhir.

Finally, I would like to express my deepest gratitude to my parents, without whom I am nothing, to provide me great opportunities, everlasting support, big encouragement and lots of love.

July, 2015


(Shivani Jindal)

Place: Thapar University, Patiala - 147 004

(Roll No. 301304009)

Abstract

Cadmium Sulphide (CdS) is one of the most important group II–VI based semiconductor with a direct bandgap of 2.42eV at room temperature. CdS:Tb nanoparticles have been synthesized by using Hydrothermal technique. The crystal structure and the average crystallite size of synthesized nanoparticles have been calculated by using X-Ray diffraction pattern. The morphology of nanoparticles has been studied through SEM images. The elemental analysis has been carried out by EDAX spectroscopy. The band gap of synthesized nanoparticles has been calculated by UV-Visible absorption spectra. Room temperature PL studies have been carried out to study the emission spectra of synthesized nanoparticles.

Contents

Certificate

Acknowledgement

Abstract

Chapter 1:<u>Introduction</u>	1
1.1 Nanoscience	2
1.2 Why do properties change at nanoscale	3
a) Quantum confinement	4
b) Large surface area to volume ratio	5
1.3 Properties of nano materials	6
1.4 Dilute magnetic semiconductors	7
1.5 Criteria for the selection of DMS materials	8
1.6 Cadmium Sulphide (CdS)	8
1.6.1 Crystal structure of CdS	
1.6.2 Applications	
1.7 Terbium	11
1.8 Synthesis of Nano materials	12

1.8.1 Top down approach	
1.8.2 Bottom-up approach	
1.8.3 Hydrothermal synthesis	
1.8.4 Synthesis of CdS nanoparticles	
1.9 Literature review	15
Chapter 2: <u>Characterization Techniques</u>	19
2.1 Scanning Electron Microscope	20
2.2 Transmission electron microscope	23
2.3 Energy Dispersive X-Ray Spectroscopy (EDS)	24
2.4 X-Ray Diffraction (XRD)	26
2.5 Photoluminescence Spectroscopy (PL)	27
2.6 Ultraviolet–Visible spectroscopy	28
Chapter 3: <u>Results and Discussions</u>	30
3.1 Structural Analysis	
3.1.1 X-Ray Diffraction (XRD)	31
3.2 Morphological studies	
3.2.1 Transmission electron microscope	33
3.2.2 Energy Dispersive X-Ray Spectroscopy (EDS)	34
3.3 Optical Analysis	
3.3.1 Ultraviolet–Visible spectroscopy	35

3.3.2 Photoluminescence Spectroscopy (PL)	37
Chapter 4: <u>Conclusions</u>	38
REFERENCES	41

List Of Figures

Figure 1.1: The energy levels become discrete at nanoscale	4
Figure 1.2: Surface area to volume ratio increases at nanoscale	5
Figure 1.3: Semiconductor host (blue) atoms with magnetic impurity in (red)	8
Figure 1.4: A representative diagram for the unit cell for crystal structure of CdS, showing (a) wurtzite (hcp), (b) zinc blend (cpp) and (c) rock salt (cpp) phases	10
Figure 1.5 Systematic of Top Down and Bottom Up approaches	13
Figure 1.6 Different steps involve in synthesis of CdS nanoparticles	14
Figure 2.1 Interaction of electron with matter	20
Figure 2.2 Schematic diagram of SEM	22
Figure 2.3 Schematic illustrating TEM	23
Figure 2.4 Working principle of EDS	25
Figure 2.5 Pictorial view of EDS	25
Figure 2.6 Bragg's Law of reflection	26
Figure 2.7 PL Spectroscopy setup	27
Figure 2.8 Schematic representation of principle of UV-Vis Spectrometer	29
Figure 3. 1 (A) XRD patterns of undoped and Tb doped CdS nanoparticles. (B) Enlarged view around $2\theta \sim 25^\circ$	32
Figure 3.2: TEM images of (a) undoped CdS (b) 15% Tb doped CdS nanoparticles	33
Figure 3.3: EDAX spectra of (a) undoped (b) 5 %, (c) 10 %, (d) 15 % Tb-doped CdS nanoparticles	34
Figure 3.4: UV-visible absorption spectra of undoped and Tb-doped CdS nanoparticles.	35
Figure 3.5: PL spectra of undoped and Tb-doped CdS nanoparticles.	37

CHAPTER-1

INTRODUCTION

1.1 Nanoscience

Nanoscience is the phenomena occurring in systems with nanometer dimensions. Nano is about as small as it gets in the world of regular chemistry, materials science, and biology. Nanomaterials has drawn farfetched attention in recent years because of their unique size dependent properties that has great technological impact on future generation devices. The diameter of a hydrogen atom is about one-tenth of a nanometer, so the nanometer scale is the very smallest scale. A strand of human hair is approximately 75,000 to 100,000 nanometers in diameter. The width of the head of a pin is around a million nanometers and to span the length of one nanometer, we need to arrange 10 hydrogen atoms end-to-end [1].

In 1959, at the American Physical Society, a talk called “There is plenty of room at the bottom,” was given by Richard Feynman in which he laid out some of the consequences of measuring and manipulating materials at the nanoscale. In this, Feynman laid the conceptual basics for nanotechnology, in which he predicted a day when things could be miniaturized, that is, when on a very small space a large amount of information could be programmed, and when machinery could be made significantly smaller and compact [2].

'Nanotechnology' is the emerging field of science that has attracted many because of its unique properties at nano-scale. It is the ability to observe measure, manipulate, and manufacture things at the nanometer scale which exhibit novel physical, chemical and biology properties and phenomena. Nanotechnology is considered to be the next technological revolution, following on from the first Industrial Revolution. This development of nanotechnology is due to the unique and size dependent chemical, physical, electronic, magnetic, thermal, optical, mechanical and biological properties of Nanomaterials.

Nanostructures can be characterized on the basis of the number of dimension in the nanoscale (1-100 nm) [3] as follows:

- 2-D nanostructures are confined in one direction e.g. interfaces, membranes, thin films, Multi-layers etc.
- 1-D nanostructures are confined in two spatial directions e.g. nanowires, nanotubes, DNA etc.
- 0-D nanostructures are confined in all three spatial directions e.g. nanoparticles, quantum dots etc.

1.2 Why Do Properties Changes At Nanoscale?

Microparticles transition to nanoparticles causes a number of changes in physical properties. The major factors that contribute to these changes are the increase in the surface area to volume ratio, and the size of the particle moving into the dominion where quantum confinement predominates.

The major factors by which nanoscale materials may differ from macroscale materials are:

- a) Quantum Confinement
- b) Greater surface area to volume ratio

a) **Quantum Confinement:**

At nanoscale, the electronic energy levels become discrete i.e. there is finite density of states, because of the confinement of the electronic wave function to the physical dimensions of the particles (Figure 1.1) and this phenomenon is called Quantum Confinement. When the diameter of the particle is of the magnitude as the wavelength of electron wave function, the quantum confinement comes into picture [4]. When the material size is at nano scale, their electronic and optical properties deviate significantly from those of bulk materials.

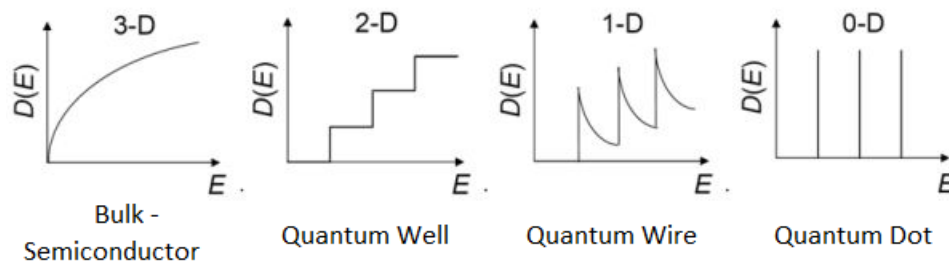
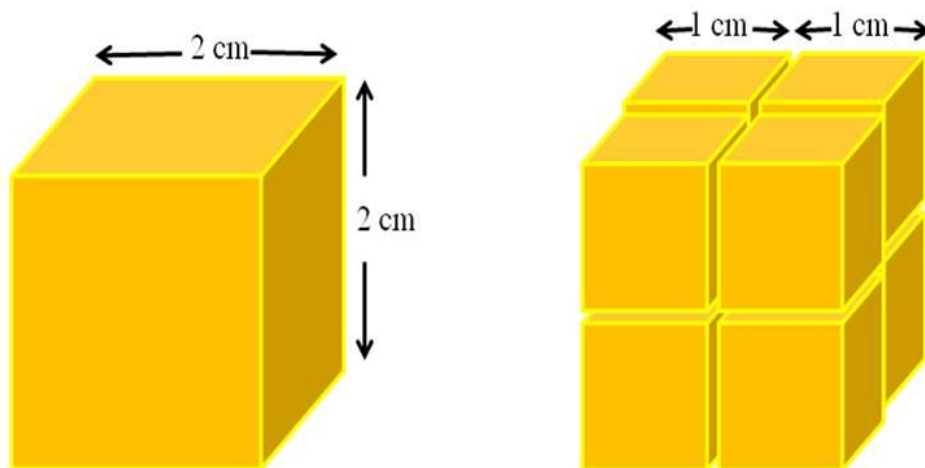


Figure 1.1: The energy levels become discrete at nanoscale

When the confining dimension is large as compared to the wavelength of the particle then particle behaves as a free particle [5]. During this state, band gap remains at its original energy due to the continuous energy state. However, with decreasing confining dimension, the energy spectrum becomes discrete, typically at nanoscale, and band gap becomes size dependent. As the size of the particle decreases, there is a blue shift in optical illumination.

b) Surface Area to Volume Ratio:

Surface to volume ratio (SA/V) is important concept for understanding the change of properties at nano-scale. SA/V is a prerequisite for understanding of size-dependent properties and behaviors and changes that are at the core of nanoscience. Many of special properties that material exhibits at nanoscale result from the effect of size on the surface area to volume ratio (SA/V). When the reactions takes place at the surface of a chemical or material, the greater the surface area to volume ratio the greater the reactivity.



# of Cube (s)	Dimensions (cm)	Surface Area ($l \times l \times 6 \text{ cm}^2$)	Volume ($l \times l \times l \text{ cm}^3$)	Surface Area/Volume ratio
1	2 x 2	$(2 \times 2 \times 6) = 24$	$(2 \times 2 \times 2) = 8$	3
8	1 x 1	$8(1 \times 1 \times 6) = 48$	$8(1 \times 1 \times 1) = 8$	6

Figure 1.2: Surface area to volume ratio increases at nanoscale

1.3 Properties of Nanomaterials:

Nanomaterials possess different and unique properties as compared to their bulk counterpart. The properties of nanomaterials include enhanced diffusivity, reduced density, higher electrical resistance, increased strength, lower thermal conductivity etc. in comparison with bulk materials. Amongst the nano and bulk scale the properties exhibited by them are entirely different and this feature characterizes them. There is a lot of research in order to investigate these properties and also to understand their fundamentals. The reasons of existing physical properties of nanomaterials are generally related to different origins such as greater surface to volume ratio, high surface energy, quantum confinement, high reactivity, reduction in imperfections etc.

- (1) Due to huge amount of atoms present at the surface in the nanomaterials, they are highly reactive and hence, accordingly possess considerably lower melting point or phase transition temperature and also, significantly compact lattice constants.
- (2) Mechanical properties of nanomaterials are higher than that their bulk counterpart by one or two orders of magnitude. This remarkable enhancement in mechanical strength is attributed to reduction in the probability of defects at nanoscale.
- (3) Optical properties at nanoscale are wholly different from that of its bulk counterpart. In semiconductor nanoparticles, the optical absorption peak shifts towards shorter wavelength, results in the increase in band gap, which causes variation in the color of metallic nanoparticles with the changing size due to the phenomena known as Surface Plasmon Resonance.
- (4) A decrease in electrical conductivity of nanomaterials with reducing dimensions to nano scale is owed to increasing surface scattering whereas it has also been found to improve appreciably, due to the better ordering in microstructures, such as in polymeric fibrils.

(5) Magnetic properties of nanostructured materials are different from that of their bulk counterpart. Ferromagnetic behavior in bulk materials transfers to super paramagnetism at the nanometer scale owing to the huge surface energy.

(6) An intrinsic thermodynamic property of nanostructures and nanomaterials is self-purification. Heat treatment results in increasing the diffusion of impurities and intrinsic structural defects dislocations.

So, all these properties are size dependent. In other words, properties of nanostructured materials can be changed considerably by varying the shape, size or extent of agglomeration.

1.4 Dilute magnetic materials(DMS):

Any semiconductor in which a part of lattice is replaced by magnetic ions can be regarded as a dilute magnetic semiconductors. These materials are also known as semimagnetic semiconductors (SMSC) or dilute magnetic semiconductor (DMS). These semiconductor alloys consists of two interacting sub-systems. The first of these, is the system of delocalised valence and conduction band electrons. The second is, diluted system of localised magnetic moments associated with the magnetic atoms. The most commonly used DMS are II–VI compounds (ZnS, CdSe, CdS, etc.), with rare earth elements (e.g. Tb, Gd, Eu) and transition metal ions (e.g. Mn, Fe, Co) substituting their original cations. There are also material based on IV-VI (e.g. PbTe, PbMnTe, SnTe) and recently III–V (GaAs, InSb) crystals.

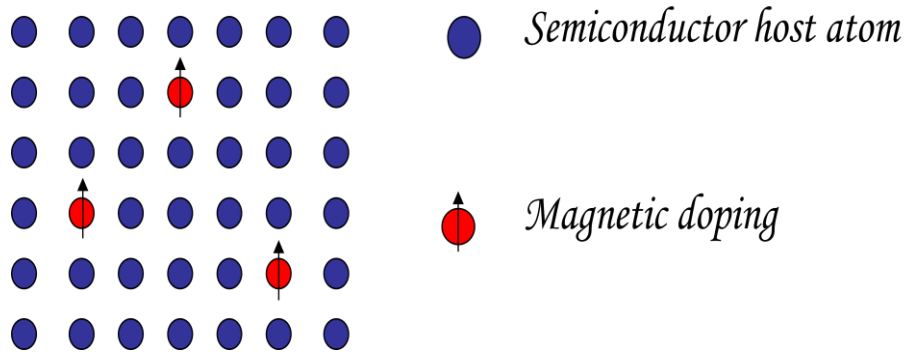


Figure 1.3: Semiconductor host (blue) atoms with magnetic impurity in (red)

Diluted magnetic semiconductor (DMS) are one of the most promising candidates for spintronic applications. For practical applications, DMS material should be ferromagnetism at room temperature.

1.5 Criteria for the selection of DMS materials:

Two major criteria to select the most promising materials for semiconductor spintronics are given as follows:

- Ferromagnetic behavior at room temperature.
- A major advantage would be there if an already existing technology becomes base for the material in other applications.
-

1.6 Cadmium Sulphide (CdS):

Cadmium Sulphide (CdS) is the II–VI based semiconductor having a direct band-gap of 2.42eV at room temperature and has been extensively used in making electronic and opto-electronic devices[7]. This has widespread application in various technical fields that includes photochemical catalysis, gas sensor, detectors for infrared and lasers, the photoconduction and

electroluminescent properties of cadmium sulfide have been applied in manufacturing of consumer goods [8].

Physical properties of CdS:

Molecular formula	CdS
Physical state and appearance	Solid(Solid powder)
Molecular Weight	144.46 g/mole
Band Gap	2.42eV
Color	Yellow
Melting Point	Sublimes (980°C or 1796°F)
Specific Gravity	4.82 g/cm ³
Solubility in water	Insoluble in hot and cold water

1.6.1 Crystal structure of CdS:

It can attain three types of crystal structures namely wurtzite, zinc blend and high pressure rock-salt phase(Figure 1.4). Among these, wurtzite is the most stable structure and is easy to synthesize. Wurtzite phase have been observed in both the bulk and nano-crystalline CdS while cubic and rock-salt phases are observed only in nano-crystalline CdS [9][10]. The wurtzite form comprises of hexagonal close packing (hcp) in which the stacking sequence of the atoms is ABABAB..., while, the zinc blende and rock salt structure have the stacking sequence of the atoms as ABCABCA..., i.e., called cubic close packing (ccp). In hexagonal wurtzite and cubic zinc blend, each atom is coordinated to four other atoms in tetrahedral fashion such that each atom has four neighboring atoms of the opposite type [11], whereas in rock-salt each atom is

coordinated to six other atoms in octahedral fashion such that each atom has six neighboring atoms of the opposite kind.

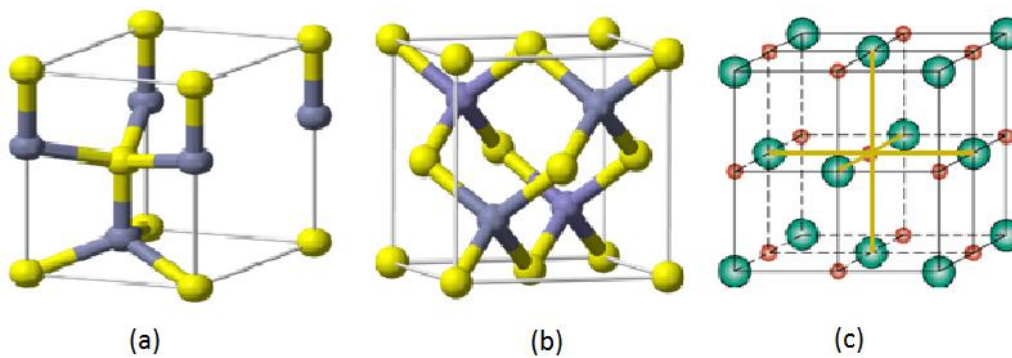


Figure 1.4: A representative diagram for the unit cell for crystal structure of CdS, showing (a) wurtzite (hcp), (b) zinc blend (ccp) and (c) rock salt (ccp) phases.

The nanoparticles of CdS show unique physical, chemical and structural properties from the bulk. The melting point, electronic absorption spectra, band gap energy, crystal structure, and other properties of cadmium sulphide nanoparticles (CdS-NP) are affected by size [12] [13].

1.6.2 Applications:

CdS is a significant visible-light-sensitive semiconductor, which makes it possible to utilize solar energy efficiently. CdS has been extensively used for photocatalytic splitting of water for hydrogen production [60] and for photo degradation of organic or inorganic pollutants in air and water [61] under visible light (VL) [14].

Because of the larger value of band gap (E_g), CdS is widely studied as it allows light emission between blue and red wavelengths. Due to the large band gap of CdS nanoparticles, it is used as window material in hetero-junction solar cells. CdS is used as n-type material along with p-type

materials like gallium-arsenide, indium-phosphide and cadmium-telluride in p-n junction solar cells [15].

1.7 Terbium:

Terbium is the member of the lanthanide group of the periodic table and is a silver-grey, ductile, soft, malleable metal. It is stable in air, but it is slowly oxidized [16] and it can react with cold water. It is one of the rare earth elements, although is twice as common in the Earth's crust as silver. It is reasonably stable in air, and has two crystal allotropes that have transformation temperature of 1289°C [17]. It is contained in many minerals but not found as free element in nature and its ores are cerites, bastnasite and monazite.

The Terbium (III) cation in a bright lemon-yellow color has brilliant fluorescent property, due to which a strong greenish emission line in combination with other emissions of orange and red are observed. The yttrium-fluorite variety of the mineral fluorite owes its creamy-yellow fluorescence in part to terbium.

The physical properties of Terbium are listed below:

Name	Terbium
Symbol	Tb
Element category	Lanthanides
Phase	Solid
Density	8.23 g-cm ⁻³
Liquid Density at melting point	7.65 g-cm ⁻³
Melting Point(M.P)	1629K

	(1365°C, 2473°F)
Boling Point(B.P)	3503K (3230°C, 5846°F)
Heat of fusion	10.51 kJ-mol
Heat of vaporization	293
Specific heat capacity	(25°C) 28.91 J-mol

1.8 Synthesis of Nano materials:

There are two basic approaches for synthesis of nanomaterials i.e. top down approach and bottom up approach.

1.8.1 Top down approach:

A top down approach involves the splitting up of massive portions of solids into smaller portions. This approach may involve milling or attrition, chemical methods and volatilization of solid followed by condensation of volatilized components. The biggest problem with this approach is increase in imperfection of the surface structure. This increase in surface imperfection causes reduction in conductivity due to inelastic surface-scattering and this results in generation of excessive amount of heat, which makes designing and fabrication much more challengeable task.

Examples of top down approach:

1. Optical and X-Ray lithography
2. Scanning probe lithography
3. Vapour phase condensation

1.8.2 Bottom-up approach:

A bottom-up approach involves the making of material atom by atom or molecule by molecule or cluster by cluster. Nanostructures obtained with this approach are with less defects, have more homogeneous chemical composition because of the reduction of Gibbs free energy, so that the obtained nanostructures are in state to thermodynamic equilibrium state.

Examples of bottom-up approaches:

1. Sol-gel
2. Chemical co-precipitation
3. Self-assembly
4. Micro-emulsion

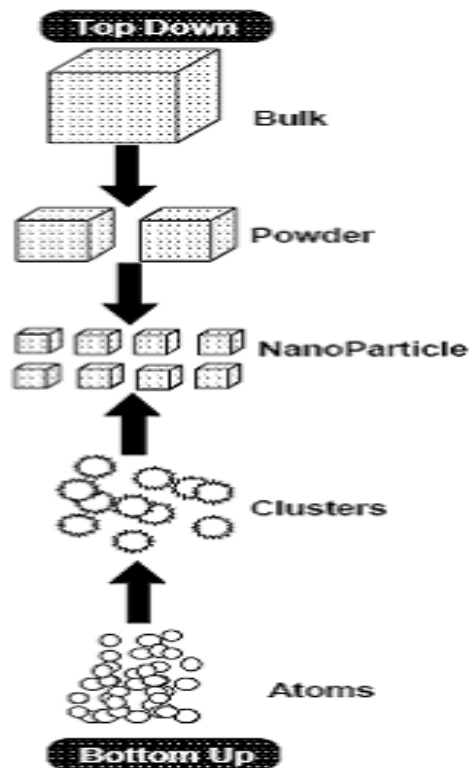


Figure 1.5: Systematic of Top Down approach and Bottom Up approach

1.8.3 Hydrothermal Synthesis:

Hydrothermal -synthesis includes different techniques of crystallizing substances from high-temperature aqueous solution at higher vapor pressure and also termed as "hydrothermal method".

Hydrothermal synthesis is basically the Bottom-Up approach in which there is the synthesis of single crystals. It is typically carried out in an apparatus that have steel-pressure vessel, which is called Autoclave. Between the opposite ends of the growth chamber, temperature gradient is maintained i.e. at hotter end solute dissolves and at cooler end it is deposited on seed crystal[18].

1.8.4 Synthesis of CdS nanoparticles:

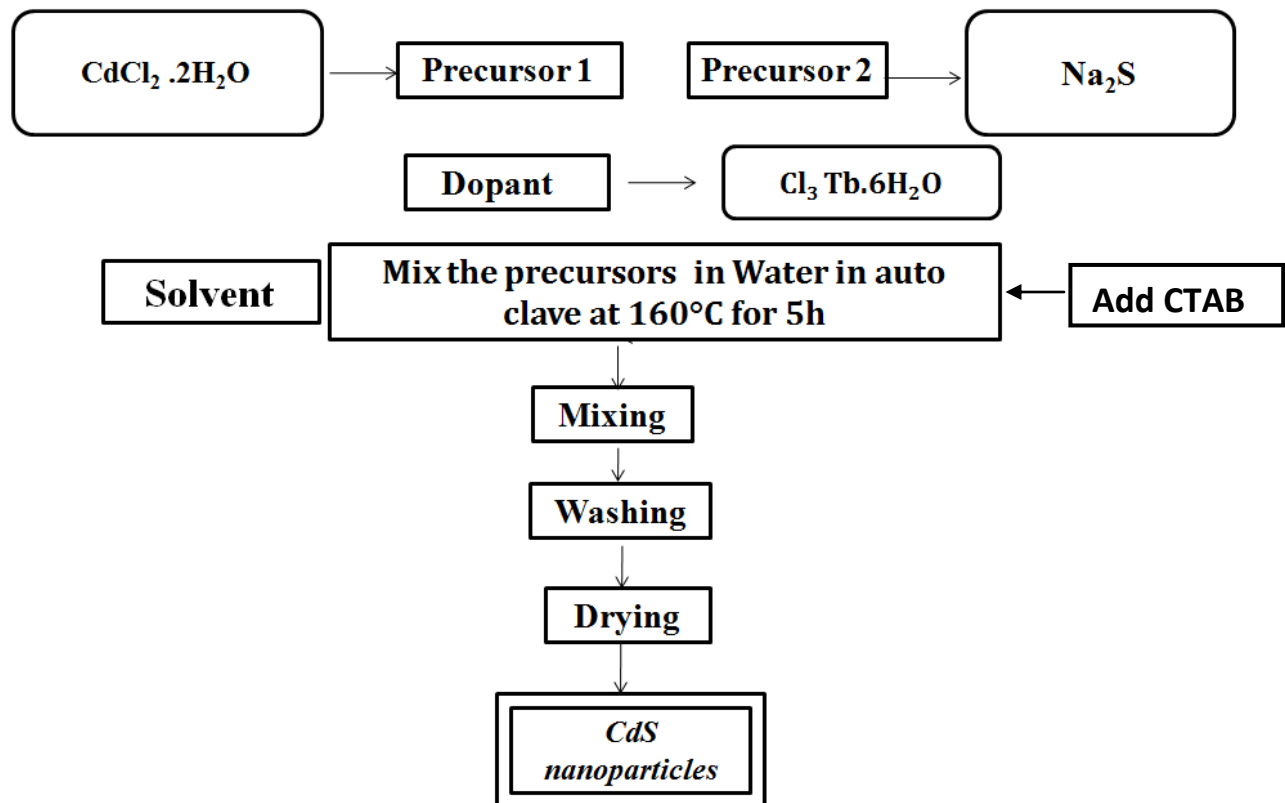


Figure 1.6: Different steps involve in synthesis of CdS nanoparticles

Pure and Tb-doped Cadmium Sulphide(CdS) nano-particles have been synthesized by using Hydrothermal technique. For synthesis of CdS nanoparticles, 0.25 M cadmium chloride ($\text{CdCl}_2 \cdot 2\text{H}_2\text{O}$) has been dissolved in water. The stoichiometric amount(0.25 M) of sodium sulphide (Na_2S) and 0.05mg of Cetyl Trimethyl Ammonium Bromide (CTAB) has been added in the above-mentioned solution, and stirred for about 30 min. The solution is then put into a Teflonlined stainless steel Autoclave. Then this autoclave is sealed and placed in a furnace maintained at temperature 160°C for 5h to get CdS nanoparticles. The precipitates of CdS nanoparticles are collected washed with distilled water and ethanol for several times to remove impurities. The samples are finally dried in hot air to obtain the powder. Similar method has been adopted for the synthesis of Tb-doped $\text{Cd}_{1-x}\text{Tb}_x\text{S}$ nanoparticles with different molar concentration 5, 10, 15%.

1.9 Literature Review:

The literature was reviewed in detail, in order to learn and gather optimum information as to the genesis and the technical applications of the work and is given as under:

In 1960, there was a category of materials which was generally called as Concentrated magnetic semiconductors and semimetals, which are as CrBr_3 ($T_C = 37 \text{ K}$), CdCr_2S_4 ($T_C = 84.5 \text{ K}$), HgCr_2Se_4 ($T_C = 106 \text{ K}$), CdCr_2Se_4 ($T_C = 130 \text{ K}$), EuX ($X : \text{O, S, Se, Te}$), Fe_3O_4 , CrO_2 ($T_C = 400 \text{ K}$), BiMnO_3 ($T_C = 105 \text{ K}$), SeCuO_3 ($T_C = 26 \text{ K}$), YTiO_3 ($T_C = 29 \text{ K}$), EuO ($T_C = 79 \text{ K}$) and Semimetals: MnAs , MnSb , CrAs , CrSb ; semimetals–double perovskites $\text{A}_2\text{BB}'\text{O}_6$: $\text{Sr}_2\text{FeMoO}_6$ ($T_C = 420 \text{ K}$), $\text{Sr}_2\text{CrReO}_6$ ($T_C = 635\text{K}$), $\text{Sr}_2\text{CrReO}_6$ ($T_C = 620 \text{ K}$), $\text{Sr}_2\text{FeMoO}_6$ ($T_C = 416 \text{ K}$).

In the 1960s and early 1970s Eu-based chalcogenide materials were studied greatly as they which exhibited ferromagnetism with Curie temperature of about 50 K or less. But problem with these were that they have poor semiconducting properties [19].

In 1980s there was other class of II–VI ternary and quaternary semiconductor alloys which were magnetically doped, (CdT)Se, (CdT)Te, PbSnMnTe ($T = \text{Fe}^{2+}, \text{Co}^{2+}, \text{Mn}^{2+}$), $\text{Cd}_{1-x}\text{Mn}_x\text{Te}$, ($T_C < 10$ K); spin glasses, antiferromagnets, paramagnets, but problem with these was that they have very low curie temperature (5K) [20].

In 1990, new category Semimagnetic semiconductors was introduced, $A^{\text{II}}B^{\text{VI}}$ and $A^{\text{IV}}B^{\text{VI}}$ hosts ($A^{\text{II}} = \text{Zn}, \text{Cd}, \text{Hg}$; $A^{\text{IV}} = \text{Pb}, \text{Sn}$; $B^{\text{VI}} = \text{S}, \text{Se}, \text{Te}$) such as II-VI (ZnMnSe, ZnCrTe, ZnCrSe, CdMnTe, CdMnSe), IV-VI (PbMnTe, (Pb, SnMn)Te), VI (GeMn, SiMnC), Oxides (ZnO, TiO_2 , SnO_2 , Cu_2O), (CdGeMnP₂, ZnGeMnP₂, ZnSnMnAs) [21-22].

In 2000 there comes class of Diluted magnetic semiconductors which includes III–V hosts (Ga,Mn)As [23-24] ($T_C \sim 170$ K), (In,Mn)As [25] ($T_C = 60$ K), (Ga,Mn)P [26] ($T_C = 400$ K), (Ga,Mn)N [27] ($T_C = 940$ K). But these materials have problem that magnetic transition metal (i.e. Mn) is not thermodynamically stable in the semiconductor host and tends to segregate [28] [29] due to which there making become difficult. There are also many reports in literature on the doping with other transition metal ions in III-nitride materials, such as Mn-doped AlN [30], Cr-doped GaN [31–32], Cr-doped AlN [31, 33, 34], Co-doped GaN [35], Fe-implanted p type GaN epilayer [36], Gd-doped GaN films [37], and Vanadium (V) doped GaN [35]. Moreover, for the III–V DMSs, the ferromagnetism with T_C often above room temperature has been found in several other DMSs, including $\text{Ge}_{1-x}\text{Mn}_x$ [38], $\text{Cd}_{1-x}\text{Mn}_x\text{GeP}_2$ [39], $\text{Ti}_{1-x}\text{Co}_x\text{O}_2$ [40], and $\text{Zn}_{1-x}\text{Co}_x\text{O}$ [41].

In the end of 1990s by using molecular beam epitaxy(MBE) films were grown. Now it becomes possible to go beyond solubility limit with these newly developed techniques like MBE, MOCVD, CVD, rf-sputtering. The major negative aspect is that these techniques are very costly, time consuming process, required high purity precursors, and high vacuum system for the growth [42].

Rare-earth and transition-metal-doped II-VI semiconductors such as CdS[43-44-45], ZnS[48], CdSe[46-47],ZnSe[49],CdTe and ZnTe are current interest of research, because of their unique optical and magnetic properties.

CdS is widely used in photo-luminescence (P.L) and electro-luminescence applications. There is a lot of literature available on photo-luminescence and structural-properties of CdS nanoparticles [43-44-45].

Luminescence process occurs when at appropriate external excitation, an Electro-magnetic radiations are produced by a substance. CdS is greatly used for opto-electronic applications in laser-light- emitting diodes and many other optical devices [50]. To alter the properties of chalcogenides in positive way, these are doped with various materials. Doping of CdS nanoparticles is done to improve their photoluminescent properties. To enhance the properties of chalcogenides they have been doped with rare earth metals, i.e., Europium, Terbium, Yttrium etc.

Tiseaun et al.(2003) [51] have studied the optical properties of Tb doped thio-salicylic- capped CdS nano-crystals and made comparative study of time resolved photo-luminescence properties of thio-salicylic- capped CdS and ZnS nano crystals doped with Tb.

C.Tiseanu et al. (2003) [52] reported the optical properties of thio-salicylic-capped CdS nano-crystals which are doped with Tb.

Hua et al. (2006) [53] has reported the doping of terbium in ZnS. They have synthesized the Tb doped ZnS nano-crystals of size of about 3-4 nm by using Co-precipitation reaction technique and studied the electro-luminescent properties.

Jyothy et al. (2009) [54] has studied Tb³⁺/CdS nanoparticles doped silica xerogels and studied its fluorescent properties. In presence of CdS nano-particles there is strong 4f⁸→4f⁷5d transition band of Tb in excitation spectrum. By co-doping of CdS nanoparticles, the fluorescence intensities of Tb³⁺ ions are greatly enhanced.

S. Rai et al. (2010) [55] prepared terbium doped CdS nanoparticles and studied its photoluminescence spectra. They observed enhancement in luminescence of Terbium doped CdS nanoparticles that are embedded in SiO₂ amorphous matrices. By varying the CdS concentrations and annealing temperature there is change in luminescence characteristic.

CHAPTER- 2

CHARACTERIZATION

TECHNIQUES

Characterization Techniques

The characterization of nano-materials plays very important role to know their structural, morphological, optical, magnetic, compositional, electrical and chemical properties. These characterizations are done using different characterization techniques that includes X-ray diffraction(XRD) for structural analysis, Scanning electron microscopy(SEM) and Transmission electron microscopy (TEM) for morphological and compositional analysis, Photoluminescence spectroscopy and U.V- visible spectroscopy for optical studies.

2.1 Scanning Electron Microscope (SEM) :

Scanning electron microscope (SEM) uses a highly energetic beam of electrons for taking the images of sample by scanning it.

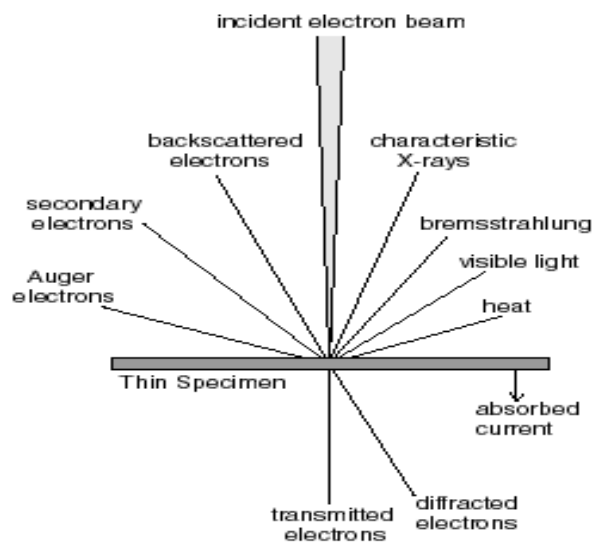


Figure 2.1: Interaction of electron with matter

A signal is produced when electrons interact with atoms and this signal has information about composition, surface topography, crystalline structure, chemical composition, orientation of

materials making up sample and other properties of sample. Interaction of electron with matter produce large number of effects as shown in fig. 2.1. Electrons under-go two types of scattering i.e. elastic and inelastic.

In **elastic scattering**, the kinetic energy and velocity of electron remain constant but its trajectory changes. This is also known as Electron Backscattering.

In **inelastic scattering**, incident electrons interact with orbital electrons of the atom in specimen due to which there is loss of energy but trajectory of incident electron is slightly changed. This produce various effects including:

- Cathodo-luminescence
- Bremsstrahlung radiation (continuum radiation)
- Characteristics X-Rays
- Phonon Excitation (Heating effect)
- Auger Electron production
- Plasmon production i.e. secondary electrons

Working principle:

In SEM, incident electron as significant amount of kinetic energy that produces various signals by electron interaction with sample when incident electrons are decelerated in solid sample. These signals contain back-scattered electrons, secondary electrons, diffracted back-scattered electrons, photons, visible light and heat. These produced signals gives information about composition, surface topography, crystalline structure, chemical composition, orientation of materials making up sample and other properties of sample.

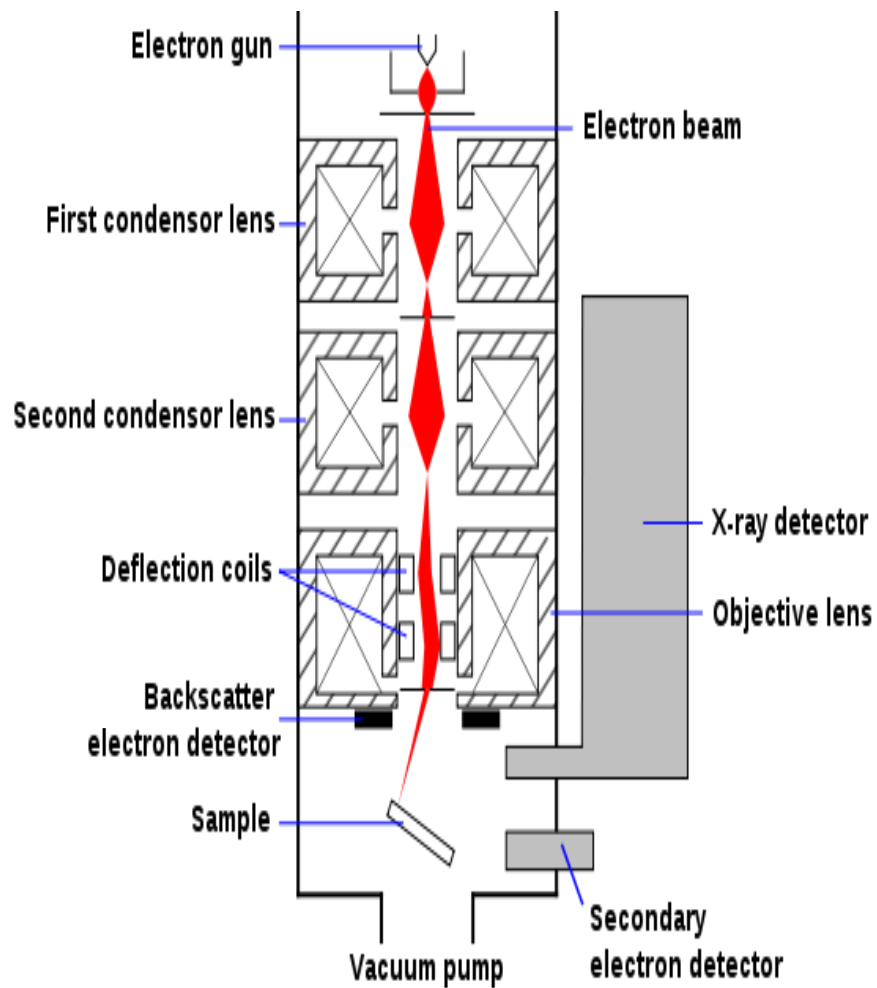


Figure 2.2: Schematic diagram of SEM

Applications:

- 1) SEM gives topographical, compositional, morphological information and in addition to this it can also detect surface fractures.
- 2) It is used to get the high resolution images of objects.
- 3) It is widely used to detect phase based on qualitative chemical analysis.

2.2 Transmission Electron Microscope (TEM):

Transmission Electron Microscope (TEM) uses a beam of electrons which is transmitted through an ultra thin specimen and electrons interact with specimen as they pass through it.

Working Principle:

When electrons are transmitted through the specimen, an image is formed due to interaction of electrons with specimen. The image is magnified and focused onto an imaging device like a fluorescent screen or photographic film layer or detected by sensors such as a CCD camera. TEMs can take images at much higher resolution as compared to those of a light microscope due to the small De-Broglie wavelength of electrons.

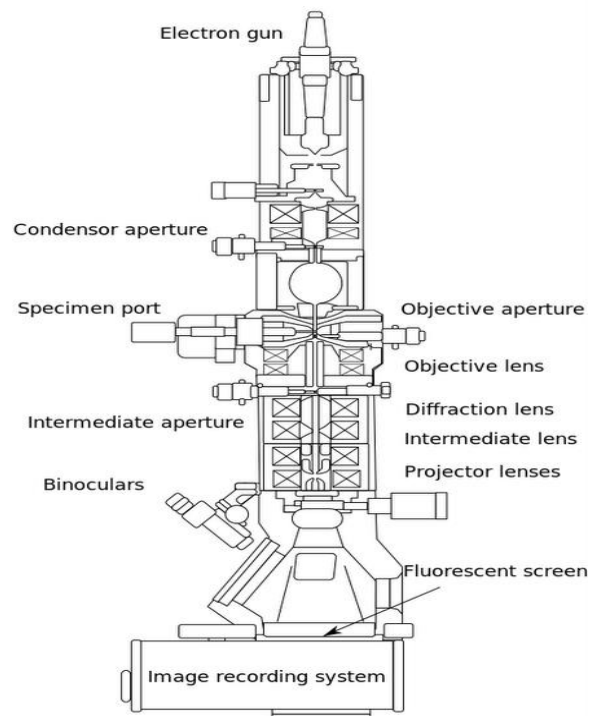


Figure 2.3: Schematic illustrating TEM

Applications:

- 1) TEMs can be utilized in many different fields like nanotechnology, medical, scientific, metallurgy, educational.
- 2) TEMs provide information of sample's morphology, composition, topography.
- 3) TEMs are used in field of semi-conductor for production and manufacturing of silicon chips and computers.
- 4) TEM images are detailed and are of high quality.

2.3 Energy Dispersive X-Ray Spectroscopy (EDS):

Energy Dispersive X-Ray Spectroscopy (EDS) is analytical technique mainly used for chemical characterization and elemental analysis of specimen. In this there is an interaction between matter and electromagnetic radiation, X-rays emitted by matter are analyzed. Each element as a unique atomic structure due to which we get different X-rays.

Working Principle:

In EDS, the electrons in the inner shell are excited by the incident beam of electrons; this causes the ejection of electron and an electron hole is formed in atomic structure. This hole is filled by electron from higher energy shell and X-Rays are released due to difference in energy between the higher and lower energy shell. These released X-Rays are analyzed by mean of Energy Dispersive Spectrometer. The detection and measurement of the X-Ray energy helps in elemental analysis because emitted X-Rays energy have characteristics of parent element and this helps in measuring elemental-composition of specimen.

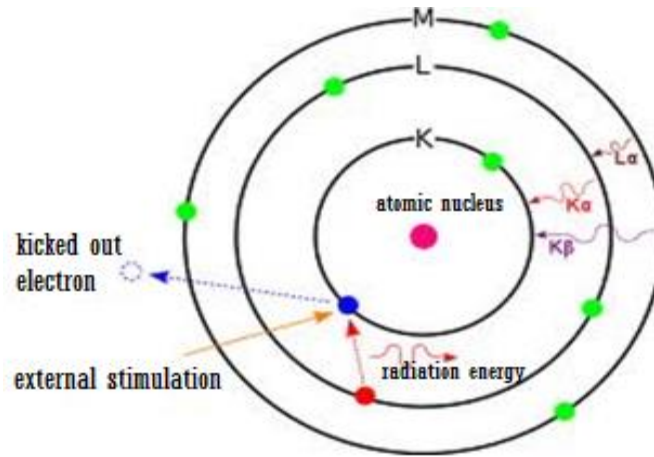


Figure 2.1: Working principle of EDS



Figure2.2: Pictorial view of EDS

Applications:

The different positions of lines i.e. peaks with an appropriate energies, gives information about composition of sample. This gives the information about contaminant present in the specimen. EDX spectra gives the relative concentrations in oxide, weight, atomic formula percentages. It can be used in various fields like home inspection, environmental testing, material identification etc.

2.4 X-Ray Diffraction (XRD):

X-Ray diffraction by crystals was studied by W.H Bragg and his son W.L Bragg and zinc sulphide (ZnS) crystals were used for this purpose. This is novel and non destructive analytical technique for quantitative analysis and identification of various crystallographic structures of materials.

Basic theory:

When incident rays fall on sample, they interact with sample and this results in constructive interference, when Bragg's law is satisfied.

Bragg's Law relates the wavelength of incident X-rays to diffraction angle and lattice spacing in crystalline sample.

$$2d\sin\theta = n\lambda$$

Where n = an integer, d = inter planar spacing, λ = wavelength of x-rays, θ = diffraction angle

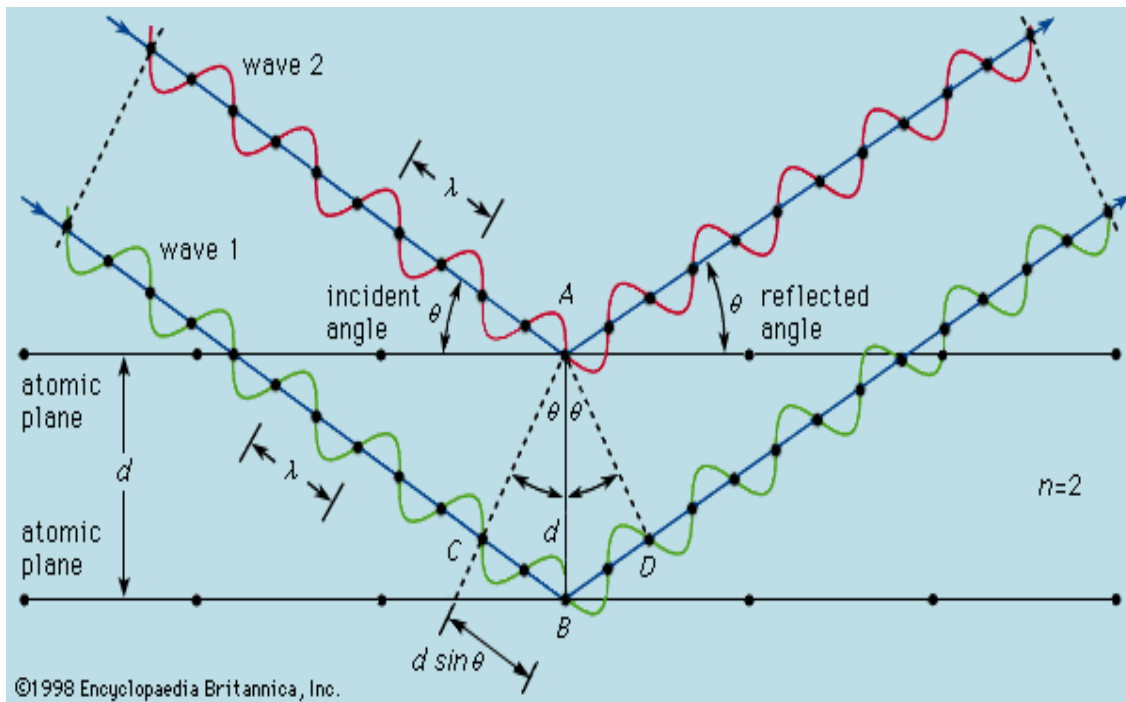


Figure 2.6: Bragg's Law of reflection

X-Ray Diffraction is used for determining:

- Crystalline phase
- Crystallite size
- Crystallite shape
- Degree of crystallinity

2.5 Photoluminescence Spectroscopy (P.L.):

Photo-luminescence spectroscopy is a non-destructive, contactless method to know the electronic structure of given sample. The samples for this can be either in liquid, gaseous or solid form.

Working Principle:

When light falls on sample, it is absorbed by sample due to which the process called photo-excitation takes place. In photo-excitation electrons jump to higher electronic state and will then returns back to lower energy state by release of energy in the form of photons. This emission of light is called photo-luminescence (P.L). Due to atomic structure difference, the various substances will emit photons of different wavelengths that can be analyzed and measured.

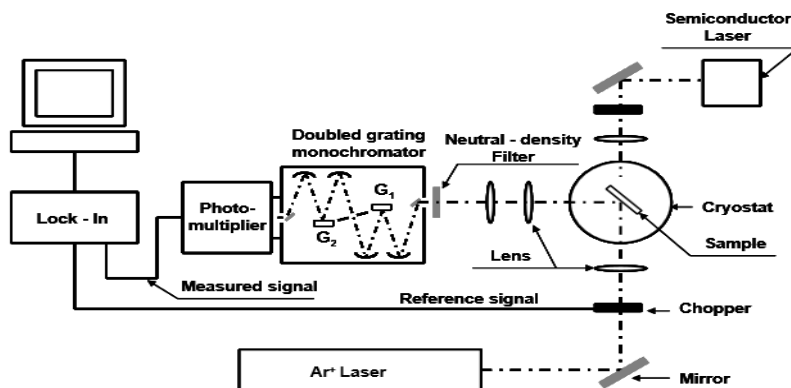


Figure 2.7: PL Spectroscopy setup

Applications:

- Impurity levels and defects detection
- Re-combination mechanisms
- Band-Gap determination
- Surface structures and excited states

2.6 Ultraviolet–Visible spectroscopy:

The Ultraviolet-Visible Spectroscopy refer to the reflectance or absorption spectroscopy in UV-visible spectral region. It uses the light in visible and adjacent i.e. U.V and near infrared ranges. Molecules undergo electronic transition in this region that is complementary to fluorescence spectroscopy. The absorption of light occurs very quickly in femto-second time scale. According to Plank's Law energy is expressed as:

$$E = h\nu = \frac{hc}{\lambda}$$

where E is energy, ν is frequency, λ is wavelength of incoming photon, h is Planck's constant and c is speed of light.

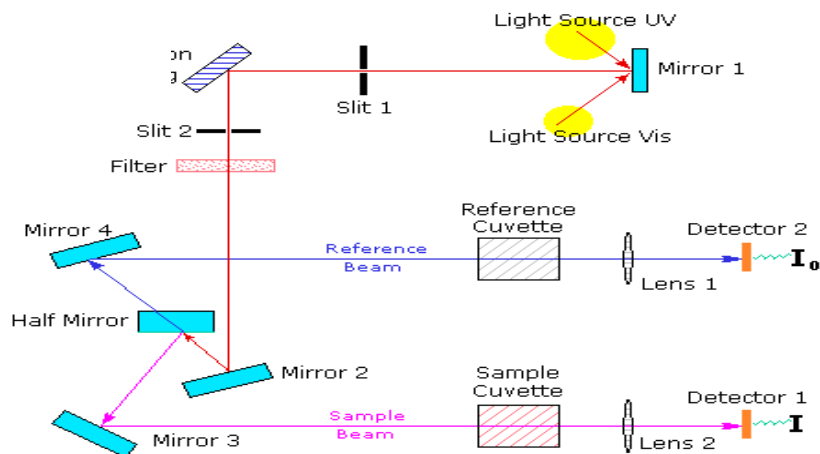


Figure 2.8: Schematic representation of principle of UV-Vis Spectrometer

The amount of light (I) that is transmitted through a solution of an absorbing chemical in a transparent solvent can be related to its concentration by Beers Law:

$$-\log I/I_0 = A = \epsilon_{\lambda}bc$$

Where I_0 is incident light intensity, A is the absorbance, b is the cell path length in cm, c is the solution concentration in moles/litre, and ϵ_{λ} is the molar absorptivity.

CHAPTER- 3

RESULTS

AND

DISSUCSSIONS

3.1 Structural Analysis:

3.1.1 X-Ray Diffraction (XRD):

Figure A of 3.1 shows the XRD(X-Ray Diffraction) patterns of synthesized nanoparticles. The diffraction peaks are sharp and highly intense indicating the high crystalline nature of the synthesized nanoparticles. All the diffraction peaks have been found to correspond to the wurtzite structure of CdS having hexagonal phase with primitive unit cell and space group P63mc(JCPDS file no. 41-1049). There is no peak corresponding to any other phase or secondary impurity of Tb. XRD pattern, confirmed the substitution doping of Tb in the host CdS. The lattice parameters (a,c) have been calculated (as shown in Table 1) from the inter-planar spacing (d) of different (hkl) planes using following relation [56]:

$$\frac{1}{d_{hkl}^2} = \frac{4}{3} \left[\frac{h^2+hk+k^2}{a^2} + \frac{l^2}{c^2} \right]$$

The crystallite size seems to be decreasing from 17.1nm to 14.0nm with the increase in the doping concentration of Tb. As we increased the dopant concentration, there is a clear shifting of peak as shown in Figure B ($2\theta \sim 25^\circ$). The ionic radii of CdS (0.97Å) is smaller than Tb (1.25Å) which leads to the shifting of the peak towards the lower diffraction with increase in dopant concentration of Tb from 5% to 15% [57].

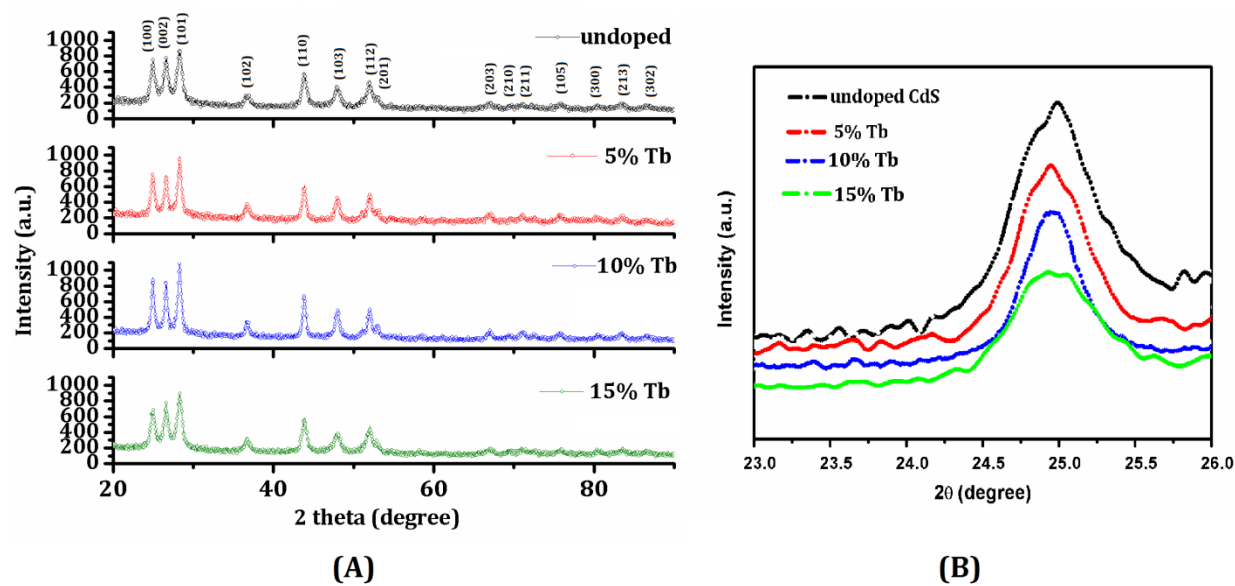


Figure 3.1: (A) XRD patterns of undoped and Tb doped CdS nanoparticles. (B) Enlarged view around $2\theta \sim 25^\circ$.

Sample Description	2θ (degree)	Lattice parameters			Crystallite size (nm)	Bandgap(eV)
		d (Å)	a (Å)	c (Å)		
Undoped CdS	26.66	3.341	4.091	6.681	15.6	2.57
5% doped CdS	26.55	3.355	4.109	6.710	17.1	2.55
10% doped CdS	26.38	3.375	4.134	6.751	18.3	2.46
15% doped CdS	26.56	3.353	4.107	6.707	14.0	2.61

Table 1: Structural parameters of undoped and Tb doped CdS nanoparticles.

3.2 Morphological studies:

3.2.1 Transmission electron microscope:

TEM images of pure and 15% Tb doped CdS nanoparticles shown in Fig.-3.2 confirms that the diameter of the synthesized nanoparticles 18 and 19 nm, respectively. In image (b) there is an extra layer which is because of the addition of CTAB during synthesis that controls the size of synthesized nanoparticles.

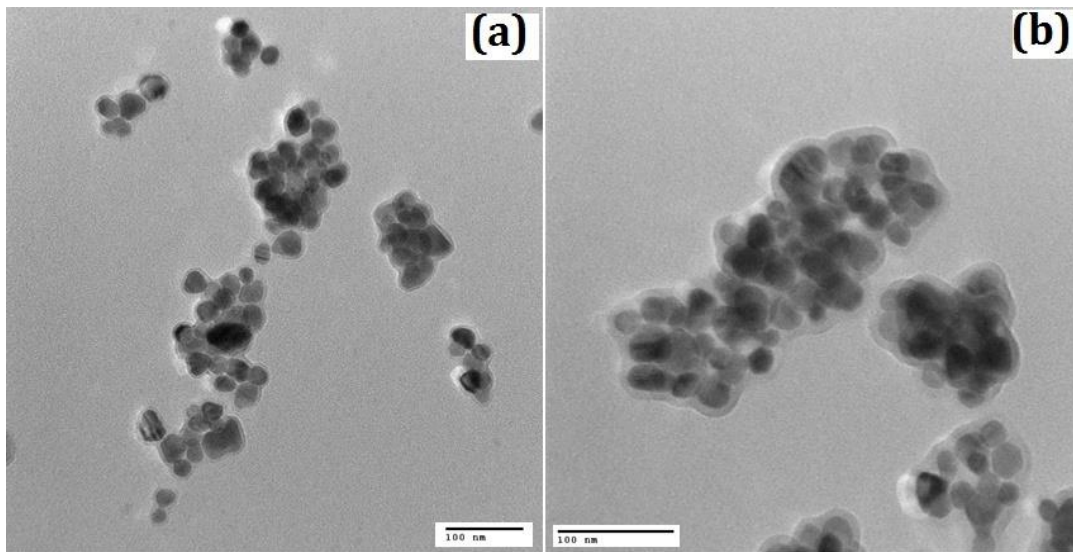


Figure 3.2: TEM images of (a) undoped CdS (b) 15% Tb doped CdS nanoparticles

3.2.2 Energy Dispersive X-Ray Spectroscopy (EDS):

Figure 3.3 (a), (b), (c) and (d) shows the EDS pattern of undoped, 5%, 10% and 15% Tb-doped CdS nanoparticles. EDS spectra show the presence of Cd, S and Tb in the synthesized nanoparticles without any other contaminant. All the elements have been found to be in their stoichiometric ratio.

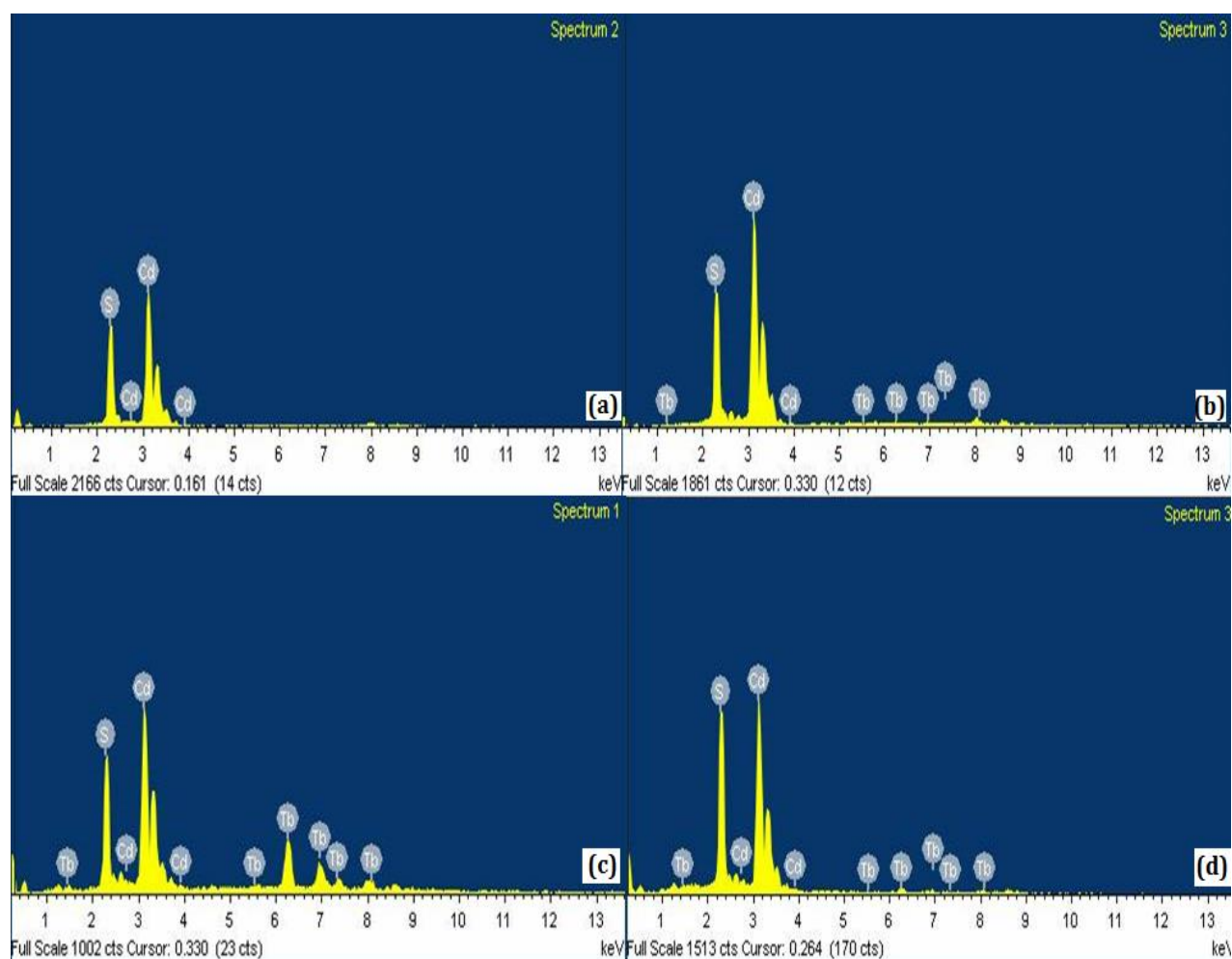


Figure 3.3: EDAX spectra of (a) undoped (b) 5 %, (c) 10 %, (d) 15 % Tb-doped CdS nanoparticles.

3.3 Optical Studies:

3.3.1 UV-visible spectra:

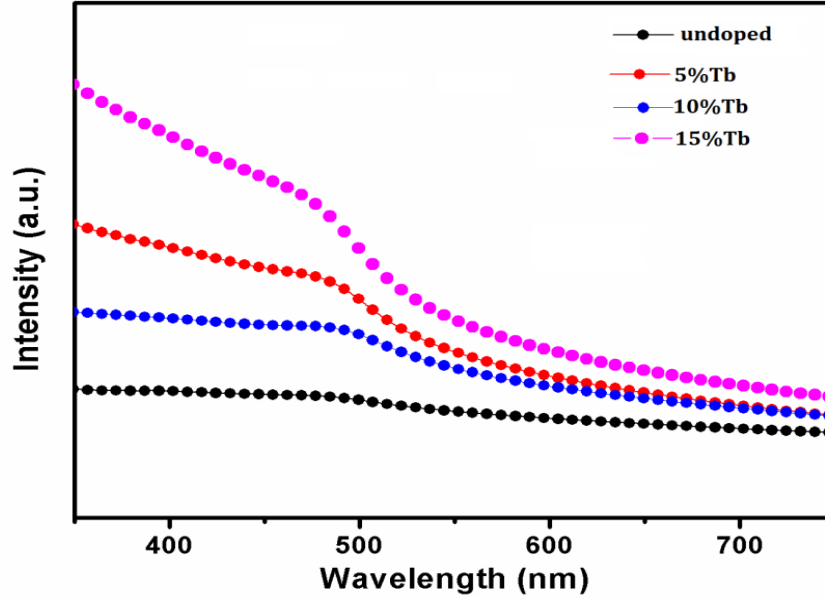


Figure 3.4: U.V- visible absorption spectra of undoped and Tb-doped CdS nanoparticles.

Figure 3.4 shows UV-visible absorption spectra of synthesized nanoparticles. The band gap energy of the synthesized nanoparticles have been calculated by using the following relation:

$$E_g = \frac{hc}{\lambda_{max}}$$

Where E_g , is the bandgap energy, h is planck's constant, c is the velocity of light, and λ_{max} is the maximum absorption of CdS nanoparticles. The bandgap of pure CdS nanoparticles has been found to be 2.57 eV, which is higher than bulk CdS, 2.4 eV, showing blue shift in the energy band due to quantum confinement effect. Quantum confinement results due to the localization of electrons and holes in the semiconductor nanocrystallites. This will lead to change in the electronic band structure of the CdS nanoparticles, and, consequently higher optical band gap

observed as compared to that of their bulk counterpart. The variation of optical band gap with Tb-doping concentration is shown in Fig. 5. In case of 5% and 10% Tb doped CdS nanoparticles there is decrease in the band gap showing the red shift in the bandgap, and, consequently the absorption edge shifts towards the higher wavelength indicates the increase in particle size, which corroborate with XRD. Also, the decrease in the band gap values is due to the new energy levels introduced in the host lattice upon doping [58-59]. But in case of 15% Tb doped CdS nanoparticles the size decreases to 14nm which in turn causes the increase in bandgap to 2.61eV because at higher doping more strain is produced in doped CdS nanoparticles which causes decrease in the crystallite size.

3.3.2 Photoluminescence spectra:

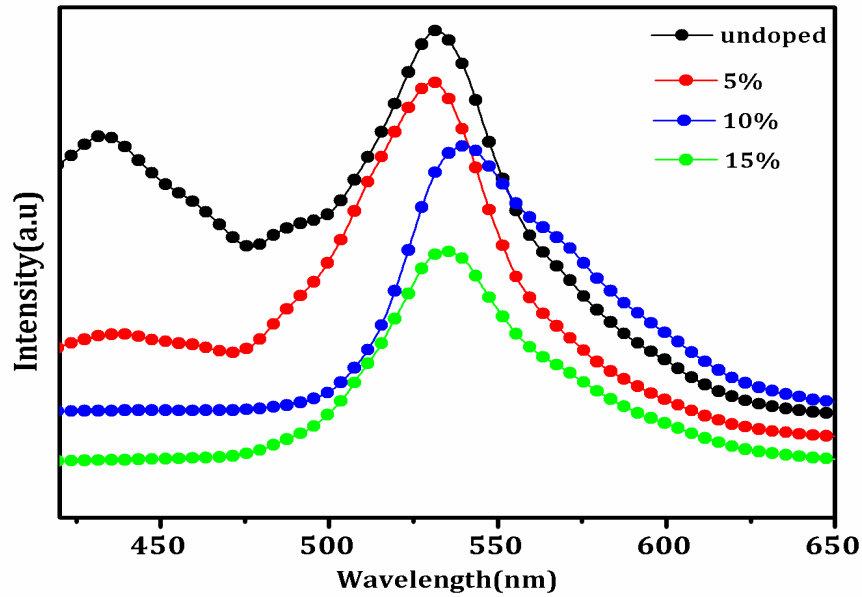


Figure 3.5: PL spectra of undoped and Tb-doped CdS nanoparticles.

Figure 3.5 shows the room-temperature photoluminescence spectra of the synthesized nanoparticles obtained at excitation wavelength 380 nm. The main excitonic emission band around 530 nm has been observed in the pure and doped CdS nanoparticles. From the emission spectra, we find a hump at 430 nm and 490 nm, which are due to blue emission. The blue shift in the optical spectrum is due to the fact that the particles in nanosize regime exhibit quantum confinement effect. The blue shift of the bandgap energy is described by effective mass approximation (Brus 1986; Kayanum1988) [54]. The peak at 540nm is due to greenish yellow emission and can be attributed to the surface related/ trap defects, due to the presence of sulphur or cadmium vacancy or interstitial. The peak at 530 nm is due to green emission.

CHAPTER- 4

Conclusions

Conclusions:

The aim of the present work was to investigate the effect of doping on the structural and optical properties of CdS:Tb. The synthesis of these nanoparticles has been carried out by hydrothermal technique with water as solvent, at 160°C for 5h. The work has been concluded as follows:

- 1) XRD analysis has been found to reveal the wurtzite phase having the hexagonal structure of nanoparticles.
- 2) TEM study has confirmed almost spherical nature of nanoparticles having average particle size of 18 nm.
- 3) EDS patterns have been found to show the presence of cadmium, sulphur and terbium without any other parasitic impurity. Hence, reveals the phase purity of the synthesized nanoparticles.
- 4) The bandgap of pure CdS nanoparticles has been found to be 2.57 eV, which is higher than bulk CdS, 2.4 eV, showing blue shift in the energy band due to quantum confinement effect.
- 5) In case of 5% and 10% Tb doped CdS nanoparticles there is decrease in the band gap showing the red shift in the bandgap. But in case of 15% Tb doped CdS nanoparticles the size decreases to 14nm which in turn causes the increase in bandgap to 2.61eV.
- 6) The main excitonic emission band around 530 nm has been observed in the pure and doped CdS nanoparticles. At 430 nm and 490 nm peaks are due to blue emission. The blue shift in the optical spectrum is due to the fact that the particles in nanosize regime exhibit quantum confinement effect.

- 7) The peak at 540nm is due to greenish yellow emission and can be attributed to the surface related/ trap defects, due to the presence of sulphur or cadmium vacancy or interstitial. The peak at 530 nm is due to green emission.

References:

- [1] S.M. Lindsay, Introduction to nanoscience, United States: Oxford University Press Inc., 2010.
- [2] http://www.openculture.com/2013/04/richard_feynman_introduces_the_world_to_nanotechnology.html
- [3] <http://www.ringsurf.com/online/2003-structures.html>
- [4] Paul Holister, Jan - Willem Weener, Cristina Roman, Tim Harper, journal of nanoparticles.
- [5] http://www.nanofm.com/terms/quantum_confinement.html
- [6] http://www.nanoed.org/lessons/Apples_to_Atoms/AtoAch5.pdf
- [7] Synthesis of CdS nanowire networks and their optical and electrical properties by R M Ma¹, X L Wei², L Dai^{1,3}, H B Huo¹ and G G Qin¹
- [7] R.M. Ma¹, X.L. Wei, L. Dai, H.B. Huo, G.G. Qin, *Nanotechnology*. 18 (2007)
- [8] P. Kavitha, S. Suseela, R.M. Mathelane, The International Journal Of Engineering And Science 2 (2013) 108-110.
- [9] V. Singh, P.K. Sharma, P. Chauhan, *Materials Characterization* 62 (2011) 43-52.
- [10] Knudson, M.; Gupta, Y.; Kunz, A. "Picosecond Electronic Spectroscopy to Determine the Transformation Mechanism for the Pressure-Induced Phase Transition in Shocked CdS," Sandia National Labs., Albuquerque, NM (US); Sandia National Labs., Livermore, CA (US), 1999

- [11] Acharya, K. P.: Photocurrent Spectroscopy of CdS/Plastic, CdS/Glass, and ZnTe/GaAs Hetero-pairs Formed with Pulsed-Laser Deposition. Ph.D. Thesis, Bowling Green State University, 2009.
- [12] R. Banerjee, R. Jayakrishnan, P. Ayyub, *Journal of Physics: Condensed Matter* 12 (2000) 10647-10654.
- [13] Y. Gogotsi, *Nanomaterials Handbook*, CRC Taylor & Francis Group, LLC: United States of America, 2006.
- [14] http://shodhganga.inflibnet.ac.in/bitstream/10603/21086/11/12_chapter3.pdf
- [15] V. Singh, P.K. Sharma, P. Chauhan, *Materials Characterization* 62 (2011) 43-52.
- [16] http://www.elementsales.com/re_exp/index.html
- [17] C.R. Hammond, "The Elements", in Handbook of Chemistry and Physics 81th edition.
- [18] https://en.wikipedia.org/wiki/Hydrothermal_synthesis
- [19] E.L. Nagaev, *Physics of Magnetic Semiconductors*, MIR, Moscow, 1983.
- [20] J.K. Furdyna, *J. Appl. Phys.* 64 (1988) R29.
- [21] T. Dietl and H. Ohno, *MRS Bulletin* (2003) 714.
- [22] V. A. Ivanov, E. A. Ugolkova, O. N. Pashkova, V. P. Sanygin, A. G. Padalko, *J. of Magn. Magn.Mater* 300 (2006) e32.
- [23] H. Ohno, A. Shen, F. Matsukura, A. Oiwa, A. Endo, S. Katsumoto, Y. Iye, *Appl. Phys. Lett.* 69 (1996) 363.
- [24] H. Ohno, *J. Magn. Magn.Mater.* 200 (1999) 110.

- [25] H. Ohno, H. Munekata, T. Penney, S. von Molnar, L. Chang, Phys. Rev. Lett. 68 (1992) 2664.
- [26] N. Theodoropoulou, A.F. Hebard, M.E. Overberg, C.R. Abernathy, S.J. Pearton, S.N.G. Chu, R.G. Wilson, Phys. Rev. Lett. 89 (2002) 107203.
- [27] M.L. Reed, N.A. El-Masry, H.H. Stadelmaier, M.K. Rytums, M.J. Reed, C.A. Parker, J.C. Roberts, S.M. Bedair, Appl. Phys. Lett. 79 (2001) 3473.
- [28] V. A. Ivanov, Bull. Russ. Acad. Sci. Phys. 71 (2007) 1610–1612.
- [29] S. Das Sarma*, E.H. Hwang, A. Kaminski, Solid State Commun. 127 (2003) 99–107
- [30] R. Frazier, G. Thaler, M. Overberg, B. Gila, C.R. Abernathy, S. J. Pearton, Appl. Phys. Lett. 83 (2003) 1758.
- [31] H. X. Liu, S. Y. Wu, R. K. Singh, L. Gu, D. J. Smith, N. Newman, M. R. Dilley, L. Montes, M. B. Simmonds, Appl. Phys. Lett. 85 (2004) 4076.
- [32] M. Hashimoto, Y. K. Zhou, M. Kanakura, H. Asahi, Solid State Commun. 122 (2002) 37.
- [33] S. Y. Wu, H. X. Liu, L. Gu, R. K. Singh, L. Budd, M. V. Schilfgaarde, M. R. McCartney, D. J. Smith, N. Newman, Appl. Phys. Lett. 82 (2003) 3047.
- [34] S. Y. Wu, H. X. Liu, L. Gu, R. K. Singh, M. V. Schilfgaarde, D. J. Smith, M. Dilley, L. Montes, M. B. Simmonds, N. Newman, Mat. Res. Soc. Symp. Proc 798 (2004) Y10.57.
- [35] J. S. Lee, J. D. Lim, Z. G. Khim, Y. D. Park, S. J. Pearton, S. N. G. Chu, J. Appl. Phys. 93 (2003) 4512.

- [36] E. Malguth, A. Hoffmann, M. R. Phillips, *J. Phys. Stat. Sol.* 26 (2008)
- [37] R. P. Davies, C. R. Abernathy, S. J. Pearton, D. P. Norton, M. P. Ivill, F. Ren, *J Chem. Eng. Comm.* 196 (2009) 1030.
- [38] N. Troullier, J. L. Martins, *Phys. Rev. B* 43 (1991) 1993.
- [39] L. Kleinman and D. M. Bylander, *Phys. Rev. Lett.* 48 (1982) 1425.
- [40] H. J. Monkhorst, J. D. Pack, *Phys. Rev. B* 13 (1976) 5188.
- [41] D. F. Shanno, K. H. Phua, *Math. Program.* 14 (1978) 149.
- [42] H. Ohno, *Science* 281 (1998) 951.
- [43] K. Kaur, G. S. Lotey, N. K. Verma, *J. Mater. Sci. - Mater. Electron.* 25 (2014) 311–316.
- [44] K. Kaur, G. S. Lotey, N. K. Verma, *J. Mater. Sci. - Mater. Electron.* 25 (2014) 2605–2610.
- [45] K. Kaur, G.S. Lotey, N.K. Verma, *Mater. Chem. Phys.* (2013) 41-46.
- [46] J. Singh, S. Kumar, N.K. Verma, *Mater. Sci. Semicond. Process.* 26 (2014) 1–6.
- [47] J. Singh, N. K. Verma, *J Mater Sci: Mater Electron* 24 (2013) 4464–4470.
- [48] G.S. Lotey, Z. Jindal, V. Singhi, N.K. Verma, *Mater. Sci. Semicond. Process.* 16 (2013) 2044.
- [49] T.J. Norman, D. Magana, T. Wilson, C. Burns, J.Z. Zhang, *J. Phys. Chem. B* 107 (2003) 6309.
- [50] J. Zhang, F. Jiang, L. Zhang, *J. Phys. Chem. B*, 108(2004) 7002-7005.

- [51] C. Tiseanu, R.K. Mehra, R. Kho, M. Kumke, *J. Phys. Chem. B*, 107 (2003) 12153-12160.
- [52] C. Tiseanu, R.K. Mehra, R. Kho, M. Kumke, *Chemical Physics Letters* 377 (2003) 131-136.
- [53] N.J. Hua, H.R. Nian, L.W. Lian, L.M. Tao, Y.T. Zhi, *J. Phys. D: Appl. Phys.* 39 (2006) 2357–2360.
- [54] P.V. Jyothy, K. A. Amrutha, J. Gijo, N.V. Unnikrishnan, *J Fluoresc.* 19 (2009) 165–168.
- [55] S. Rai, L. Bokatial, *Bull. Mater. Sci.* 34 (2011) 227-231.
- [56] B.D. Cullity, S.R. Stock, *Elementary of X-ray Diffraction*, 3rd edn. (Prentice-Hall, Englewood Cliffs, 2001)
- [57] G.S. Lotey, J. Singh, N. K. Verma, *J Mater Sci: Mater Electron* 24 (2013) 3611–3616.
- [58] Z. Jindal, N.K. Verma, *J. Mater. Sci.* 43 (2008) 6539-6545.
- [59] R. Elilarassi, G. Chandrasekaran, *J. Mater. Sci. Mater. Electron.* 24(2013) 96-105.